EFFECT OF HEAT INPUT ON THE STRUCTURE AND PROPERTIES OF ALUMINIUM WELDMENT

F. Gulshan[1] and Q. Ahsan[2]

* *fahmidagulshan@mme.buet.ac.bd*

Received: January 2013 **Accepted: May 2013**

[1] Materials and Metallurgical Engineering Department, Bangladesh University of Engineering and Technology, Dhaka, Bangladesh.

[2] Engineering Materials Department, Faculty of Manufacturing Engineering, University Teknikal Malaysia, Malaysia.

Abstract:*The probable reasons for evolution of weld porosity and solidification cracking and the structure- property relationship in aluminium welds were investigated. Aluminium plates (1xxx series) were welded by Tungsten Inert Gas (TIG) welding process, 5356 filler metal was used and heat input was controlled by varying welding current (145A, 175A and 195A). The welded samples were examined under optical and scanning electron microscopes and mechanical tests were performed to determine tensile and impact strengths. Secondary phase, identified as globules of Mg_2Al_3 precipitates, was found to be formed. Solidification cracking appeared in the heat affected zone (HAZ) and porosities were found at the weld portion. The tendency for the formation of solidification cracking and weld porosities decreased with increased welding current.*

Keywords: *Aluminium, TIG welding, welding current, secondary phase, porosity, solidification cracking*

1. INTRODUCTION

Aluminium and its alloys are widely used in fabrications [1] because of their light weight, good corrosion resistance and weldability. The unique combination of light weight and relatively high strength makes aluminium the second most popular metal that is welded. Al/Al alloy possesses a number of properties such as oxidation, solubility of gas and change in strength that make its welding different from the welding of steels. Aluminium or aluminium alloys are usually fusion welded with tungsten inert gas welding (TIG) process in which an inert gas (Ar, He) is supplied to reduce the oxidation of weld metal [2].

An increased use of aluminium in the automotive and ship building industry has resulted in renewed interest in the weldability of aluminium alloys. A large number of weldable parts in different industries often cause premature failure due to lack of proper knowledge on weldability of aluminium alloys. Even small cast parts are discarded when they encounter casting and machining defects. With improved weld deposition process most of these products may be repaired and put into the service. In addition, large and complex shape components can be manufactured by assembling small sized objects with proper joining methods.

Some of the most common problems encountered in any aluminium welds and need control are porosity, cracking and filler alloy selection [3,4]. Ductility, fatigue strength and tensile strength of welded joints are adversely affected by the inclusion of porosity. Porosity in aluminium weld originates from entrapped gases within the weld puddle. Contaminants in the shielding gas, air, and water as well as contaminants in the base or filler metals can be the origin of these gases. During welding, partially melted zone is formed immediately outside the weld, where liquation can occur and lead to hot cracking.

In the present research, a systematic investigation was made on TIG welding of aluminium alloy to improve the structure-property relationship of weldment by controlling heat input.

2. EXPERIMENTAL PROCEDURE

11 mm thick sheets of aluminium (1xxx series) were procured. The chemical composition was

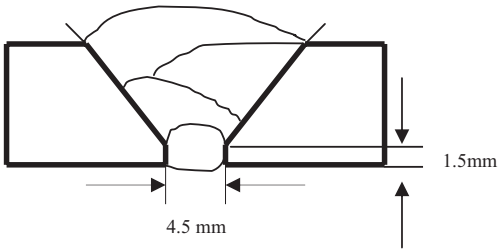

Fig. 1. Joint configuration for TIG welding

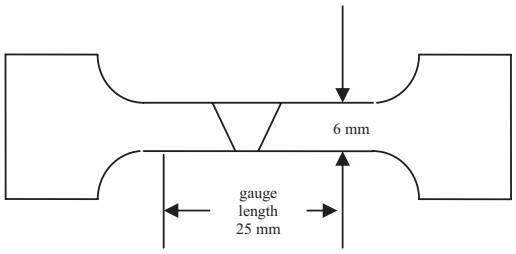

Fig. 2. Tensile test specimen

confirmed by optical emission spectroscopy (OES). Pieces measuring 35 mm x 16 mm were cut and the edges of each piece were prepared for TIG welding (Fig. 1).

The samples were rigidly clamped and welded in the flat position using 5356 filler metal (Table 1). A 1% thoriated tungsten electrode (2.4 mm diameter) was used for welding and the welding parameters used are shown in Table 2.

For metallographic investigations the specimens were longitudinally sectioned and prepared as per standard practice. The samples were etched in 15 ml HF and 10 ml HCl in 75 ml distilled water. Micrographs were recorded at weld joint, weld root, HAZ and base metal. Mechanical tests were conducted to determine tensile and impact properties of the weld zone, HAZ and also the base metal. Fig. 2 shows a typical tensile test specimen.

Charpy impact test specimens with 2 mm deep v-notch in the weld zone, in the HAZ and in the base metal were made from each weld. A typical charpy test piece is shown in Fig.3.

Table 1. Filler metal composition:

5356	**Elements**	**Mg**	**Cu**	**Fe**	**Si**	**Al**
5%Magnesium Aluminium Welding rods	**Typical Composition**	4.5-5.5%	0.10 %	0.40%	0.25%	Balance

Table 2. Welding parameters

Material	Plate No	Filler metal used	Current used (A)
Base metal- pure aluminium 1xxx series	1	5356 (Al-Mg filler)	145
	2		175
	3		195

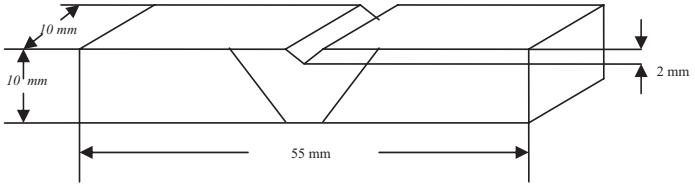

Fig. 3. Impact test specimen (Notch at Weld centre)

All fractured surfaces were observed under a scanning electron microscope. Scanning electron micrographs were recorded as secondary electron images and also as backscattered images at around 10 KV. Concentrations of the various elements present at the points of interest were determined by energy dispersive X-ray analysis (EDX) at 10 KV.

3. RESULTS AND DISCUSSION

Table 3 shows the chemical compositions of the base plate.

The optical micrographs (Fig. 4) of these plates at weld zone, HAZ and weld root show the presence of some black globular particles.

The EDX analysis of weld matrix [Fig. 5(a)] indicated the presence of only 4-5 percent Mg (the filler alloy composition) while the EDX analysis of the particles [Fig. 5 (b)] showed that the globular particles contained around 30 percent magnesium. As indicated by binary aluminium-magnesium phase diagram, the chemical composition of the precipitate particles agrees well with the composition of Mg_2Al_3. It can thus be inferred that the black particles in the micrographs were Mg_2Al_3 precipitates.

The Mg_2Al_3 precipitates are more concentrated (Fig. 4(c)) in the weld root than in the weld portion (Fig. 4(b)). This is because of higher rate of heat dissipation at the root of the weld. During welding, root pass is performed first and during solidification of this root portion heat can dissipate from all sides. So root portion cools rapidly .But the following weld passes have slow heat dissipation rate. Because during those passes, root and base metal are already preheated that slows down the cooling rate.

Micrographs of the heat affected zone of these plates show the presence of some crack lines (shown in Fig. 4(d)) that were absent in weld portion and base metal.Similar findings were reported by Lippold, et al [2], where they made an investigation of hot cracking in 5083-O Aluminium alloy weldments. Moreover Steenbergen, and Thorton [5] made a quantitative determination of the conditions for hot cracking during welding for aluminium alloys. This investigation also supports the formation of this type cracks at the HAZ. This is also supported by Huang and Kou [6] who investigated liquation cracking in the partially melted zone of full penetration welds of alloy 6061. Three welds of alloy 6061 was made with filler metal 5356 and it was found that liquation cracking occurred in these welds.These cracks form during solidification when the lowest melting point constituents (Mg_2Al_3 precipitates) are pushed to grain boundaries by the solidification fronts as the solid particles grow in size. The difference in melting point between the low melting point constituent and the bulk of the metal is

Table 3. Chemical composition of base plate

Elements	Aluminium	Silicon	***Magnesium***	Iron
Composition (Percent)	94.739	0.1584	***3.82***	0.34

Optical micrograph of plates

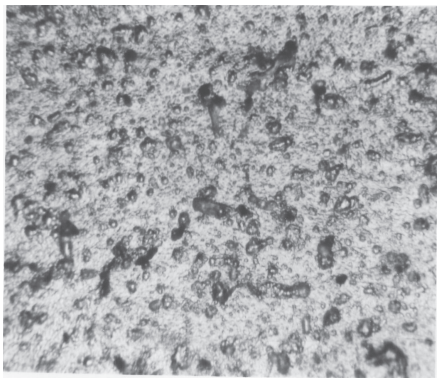

Fig. 4(a). Micrograph of plate 1
(base)

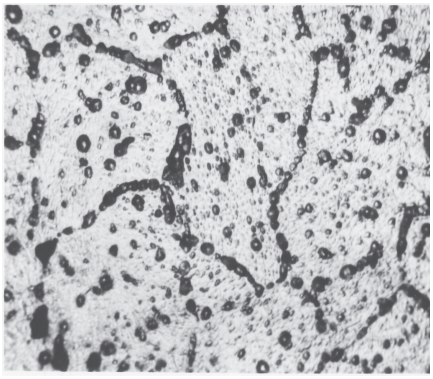

Fig. 4(b). Micrograph of plate 2
(weld portion)

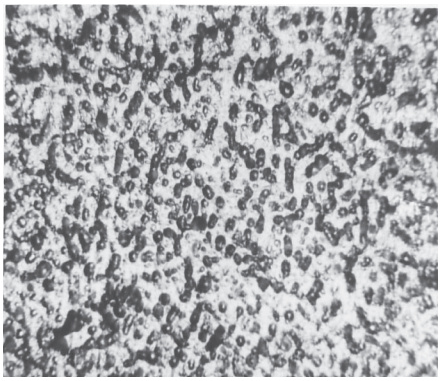

Fig. 4(c). Micrograph of plate 2 (root)

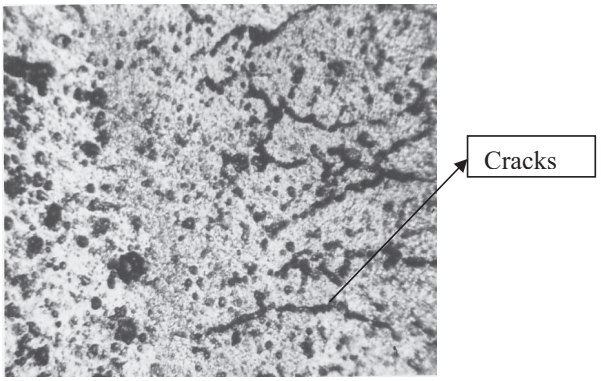

Fig. 4 (d). Micrograph of plate 2(HAZ)

sufficiently great. As a result the liquid film along the grain boundaries falls apart as the metal cools and contracts creating solidification cracking [4].

The scattered electron (SE) (Figure 6) and corresponding backscattered electron (BSE) images (Figure 7) of plates 1,2 and 3 show the presence of porosity. Gas dissolution in liquid is higher than in solid. Liquid to solid transformation rate increases with an increase in the solidification rate. As a result more gas is entrapped in solid and causes more porosity. It was found that for higher heat input (plate 3) this porosity was the minimum in quantity. This may be attributed to the fact that as heat input increases during welding, solidification process slows down, decreasing the formation of porosity [7]. Whereas at low heat input, solidification process is very fast as a result, plate 1 and 2 show the presence of excess porosity than plate 3.

SE and BSE images of plates 1,2 and 3 Location: Polished weld portion

Relationship between fractograph and mechanical properties

Impact energies and tensile properties are listed in table 4 and 5 respectively.

Table 4 shows that the impact energy at the HAZ is always higher than that at the weld portion. Because the impact properties of the HAZ are influenced by the impact property of the base plate. On the other hand, impact property at the weld portion tends to increase with an increase in heat input. It may be due to the decrease of solidification cracking at the higher heat input. An increase in heat input causes a

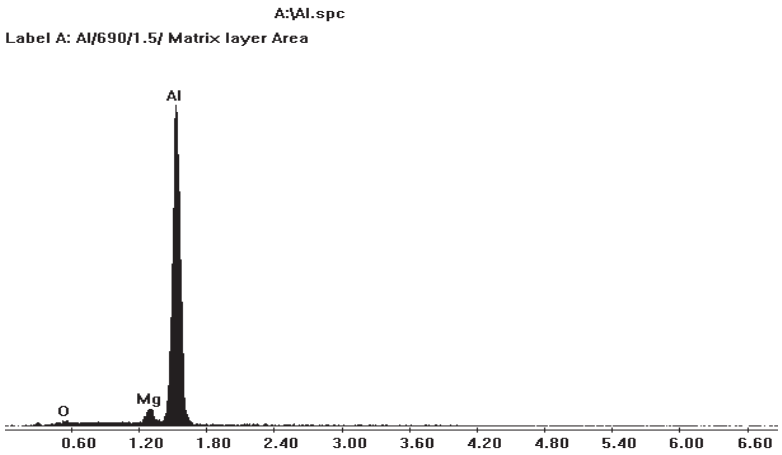

5(a)

Quantification results	
Element	**At%**
Al	95.11
Mg	4.89
Total	**100**

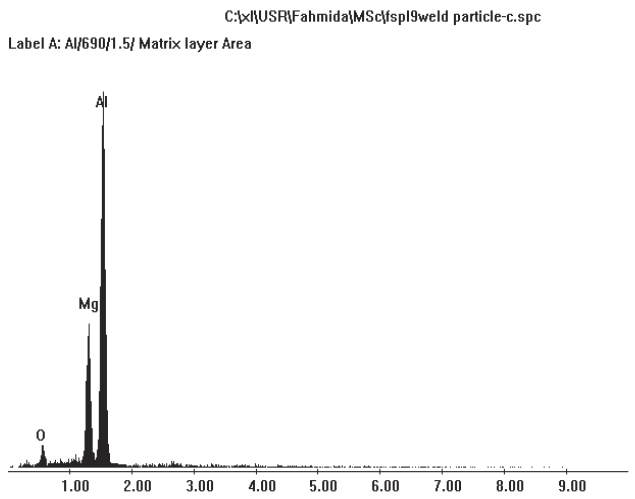

5(b)

Quantification results	
Element	**At%**
Al	70.37
Mg	29.62
Total	**100**

decrease in solidification cracking, because temperature difference between the low melting point constituents and the bulk of the metal decreases as the heat input increases. That is why plate 3 shows less solidification cracking and high impact energy. Similar observations were found by Dudas and Collins [8].

The ultimate tensile strength values of these plates (Table 5) remain almost unchanged with heat input. Figure 8 shows the fractographs of the fractured surfaces resulting from the impact tests.

The fractured surface of the weld portion and HAZ of these plates (Fig. 8(a, b,c, d)) show dimple features. The micrographs of theses plates at the weld portion and HAZ showed the presence of porosity and liquefaction cracking. This preexistence of porosity and liquefaction cracking accelerates the separation of metals during impact, resulting in decrease in impact energy than the pure aluminium plate (Table 4). On the other hand the fractured surface of the base plate (figure 8(e)) show faceted features that causes brittle fracture.

SE and BSE images of plates 1,2 and 3 Location: Polished weld portion

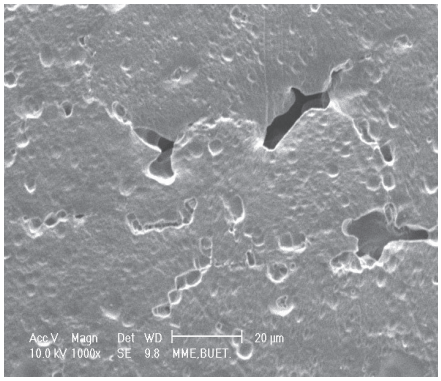

Fig. 6(a). SE image of plate 1

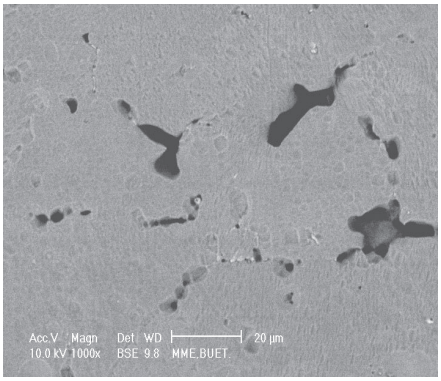

Fig. 7(a). BSE image of plate 1

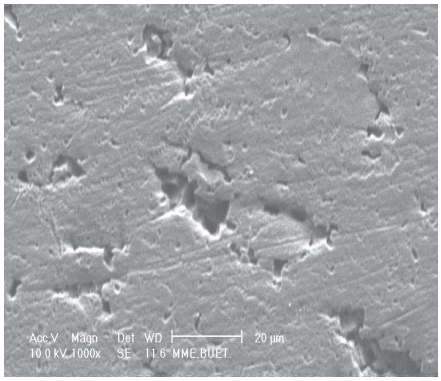

Fig. 6(b). SE image of plate 2

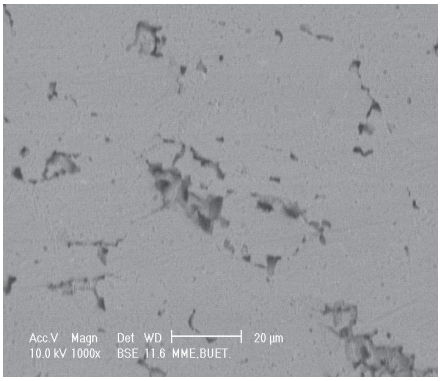

Fig. 7(b). BSE image of plate 2

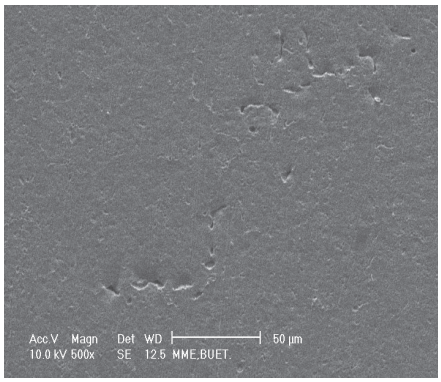

Fig. 6(c). SE image of plate 3

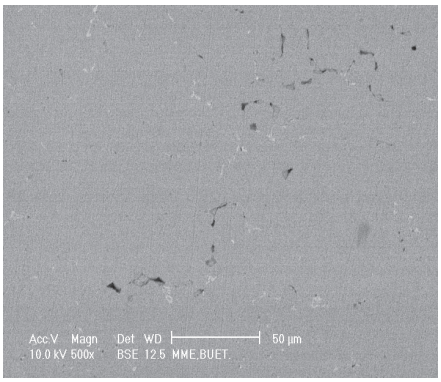

Fig. 7(c). BSE image of plate 3

CONCLUSIONS

From the results it can be concluded that:
During welding pure aluminium plates with Al-Mg filler, globules of Mg_2Al_3 precipitates were formed. The precipitates were different in size, shape and orientation at different locations of the welded samples. Solidification cracking appeared in the heat affected zone and porosities

Table 4. Impact energy values

Plate Number	Filler Used	Current used (Ampere)	Impact energy (Joules)		
			HAZ	Weld	Base
1	5356	145	48	16	82
2		175	48	20	
3		195	52	25	

Table 5. Tensile properties

Plate Number	Filler Used	Current used (Ampere)	Impact energy (Joules)		
			HAZ	Weld	Base
1	5356	145	48	16	82
2		175	48	20	
3		195	52	25	

were found at the weld portion. The tendency for these defects decreased with an increase in time for solidification after welding and with a decrease in the temperature difference between the precipitates and the bulk material.

ACKNOWLEDGEMENT

The authors are grateful to Bangladesh University of Engineering and Technolohy (BUET) for providing facilities to carry out this research work.

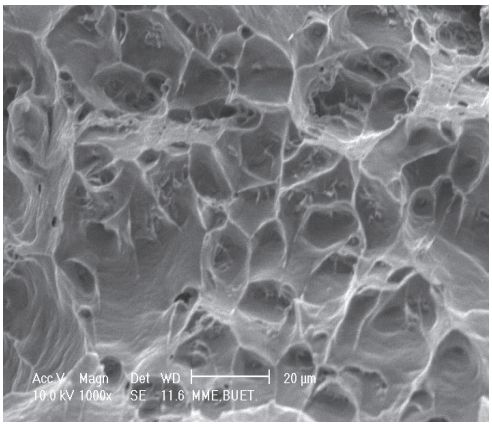

Fig. 8(a). Fractograph of plate 1 (notch at weld portion)

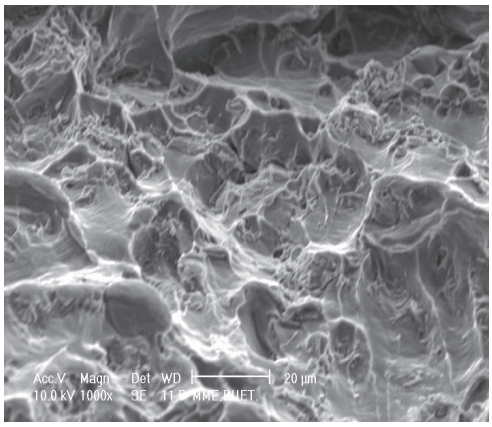

Fig. 8(b). Fractograph of plate 1 (notch at HAZ)

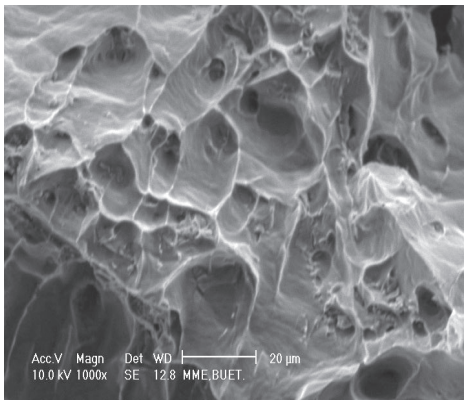

Fig. 8(c). Fractograph of plate 3
(notch at weld portion)

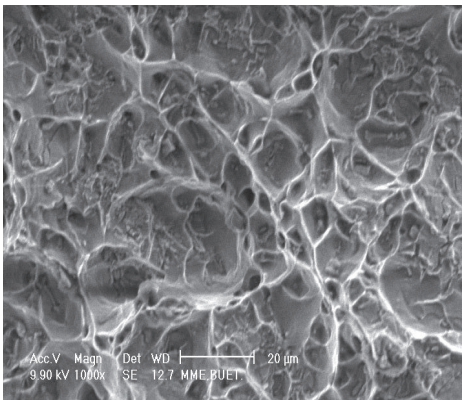

Fig. 8(d). Fractograph of plate 3
(notch at HAZ)

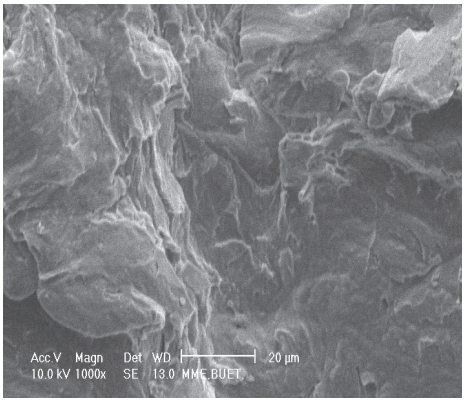

Fig. 8(e). Fractograph of base plate
Pure aluminium (1xxx series)

REFERENCES

1. Bagheri, S. M., Zamani, J. and Omrani, A. M., "A new approach to predict of mechanical properties at the interface of Aluminium/Copper explosive cladding by explosive scarf welding", Iranian Journal of Materials Science and Engineering, 2009,Vol 6 No. 4.
2. Lancaster, J. F., "Metallurgy of welding, George allen and unwin limited", London, 3rd edition, 1980.
3. Katoh, M., and Kerr, H. W., "Investigation of heat affected zone cracking of GTA welds of Al-Mg-Si alloys using the Varestraint test". Welding Journal, 1987, 66(12), 360-368.
4. Gittos, N. F., and Scott, M. H., "Heat affected zone cracking of Al-Mg-Si alloys". Welding Journal, 1981, 60(6), 95-103.
5. Steenbergen, J. E., and Thornton, H. R., "A quantitative determination of the conditions for hot cracking during welding for aluminium alloys". Welding Journal 1970, 49(2), 61-68.
6. Huang, C., and kou, S., "Partially melted zone in aluminium welds- liquation mechanism and directional solidification". Welding Journal 2000, 79(5), 113-120.
7. Eskin, D. G., Mooney, J. F., and Katgerman, I., "Contraction of aluminium alloys during and after solidification. Metallurgical and Materials Transaction", 2004, Volume 35A: 1325- 1334.
8. Dudas, J. H.,and Collins, F. R., "Preventing weld cracks in high strength aluminium alloys". Welding Journal, 1966, 45(6), 241-249.